PHYSICAL REVIEW B VOLUME 23, NUMBER 10 15 MAY 1981

Band structure, Fermi surface, Compton profile, and optical conductivity of paramagnetic chromium

D. G. Laurent and J. Callaway
Department of Physics and Astronomy, Louisiana State University, Baton Rouge, Louisiana 70803

J. L. Fry and N. E. Brener
Department of Physics, University of Texas at Arlington, Arlington, Texas 76019

(Received 9 May 1980; revised manuscript received 9 January 1981)

A self-consistent linear-combination-of-Gaussian-orbitals band-structure calculation for paramagnetic chromium employing a local exchange approximation has been performed. The density of states, Fermi surface, and x-ray form factors have been obtained and compared with available experimental data. New interpretations of some of the neutron scattering data are made, with good agreement in general for all the data. The Compton profiles and the optical conductivity have also been obtained using the full matrix element $\vec{k}$ dependence in Brillouin-zone integrations. Comparison with experiment is made for both, and correlation with experiment is good if appropriate angular averages or lifetime effects are included.

I. INTRODUCTION

The electronic structure of chromium has been under intensive investigation for a number of years, stimulated by the special magnetic structure which exists in the ground state at temperatures below 312 K. A spin-density wave of wavelength incommensurate with the observed x-ray lattice structure exists either in the form of a transverse or a longitudinal standing wave.

Theoretical models have been proposed and band-structure calculations performed to explain the structure of chromium. While Overhauser first investigated the existence of spin-density waves,[1] Lomer was the first to use Fermi-surface models to explain antiferromagnetic order in the ground state of chromium.[2] Employing energy considerations and the susceptibility function, $\chi(\vec{q})$, the possible formation of spin structures may be related to topology of the Fermi surface of a paramagnetic metal.[2-4]

In chromium, it is probable that $\chi(\vec{q})$ takes on a maximum near a value of $\vec{q}=(2\pi/a)(0,0,0.96)$, where a is the lattice constant, as a consequence of "nesting" between portions of the electron "jack" at Γ and the hole octahedron at H in the Brillouin zone (BZ). This well-known bit of Fermiology has been deduced from several experiments, referenced below, but has been examined only approximately in theoretical studies. The special topological conditions which in general can lead to singularities or maxima in $\chi(\vec{q})$ have been carefully analyzed for different Fermi-surface geometries by Roth *et al.*[5] Topological effects alone may not lead to proper predictions, since matrix-element effects can be strong.[6] A detailed numerical evaluation of $\chi(\vec{q})$ is needed to make accurate statements about the spin-density wave in chromium, but several theoretical papers lend support to the nesting interpretation in chromium without benefit of susceptibility studies.[7-11] Gupta and Sinha performed a numerical calculation of $\chi(\vec{q})$, but the accuracy of their study is in doubt because of lack of self-consistency in their augmented-plane-wave (APW) energy-band calculation.[6] Numerous studies indicate that both self-consistency and exchange have strong effects in the band structure of noble and transition metals.[8,11-15] This is made very clear in the case of chromium by the Fermi-surface figures in Ref. 11.

The accuracy and speed of various methods of energy-band theory have improved over the years since the very time-consuming work of Gupta and Sinha. More efficient methods of evaluating $\chi(\vec{q})$ are now available,[16,17] and alternative theoretical expressions for $\chi(\vec{q})$ have been derived.[18-21] A new evaluation of $\chi(\vec{q})$ incorporating these developments is warranted.

One of the purposes of this calculation is to provide an accurate band structure for paramagnetic chromium to serve as input into a calculation of $\chi(\vec{q})$. What is needed is a self-consistent band structure including exchange which gives an accurate account of available experimental data and is also suitable for use in the calculation of $\chi(\vec{q})$.

The linear-combination-of-Gaussian-orbitals (LCGO) method employed here has been developed over a period of years by these authors and others and applied to a number of crystals.[22-26] Of particular interest here are transition-metal energy-band calculations which have been done with the latest version of these computer codes and in which it has been shown that an understanding of the magnetic and electronic structure of 3*d* transition metals is possible. The important considerations are self-consistency, accurate treatment of

crystal potentials, an appropriate choice of exchange potential, and a manageable calculational procedure which provides wave functions in a convenient form for further applications. The LCGO procedures used in earlier computations for chromium,[10,11] have been improved by the addition of f orbitals to the basis, improved convergence procedures for lattice sums and a more accurate calculation of the Fourier transform of the exchange potential. This paper reports a calculation for paramagnetic chromium which has the same accuracy as recent LCGO studies of vanadium,[24] nickel,[25] and iron.[26]

The self-consistent band structure reported here is employed to determine x-ray form factors and the Compton profile is computed and compared with earlier theoretical results as well as with experimental values. A computation of the optical conductivity is then presented, including the full $\vec{k}$ dependence of momentum matrix elements.

A substantial body of data has been gathered for chromium, usually in regard to an antiferromagnetic state. This includes crystal-structure measurements,[27] magnetic-form-factor determinations,[28-31] optical studies,[31-35] neutron scattering studies of phonons,[36-38] Compton profiles,[39-40] x-ray form factors,[41-43] magnetic susceptibilities and other magnetic field experiments,[44-47] and investigation of the effects of alloying upon the properties of chromium.[32,48] This list of references is not intended to be complete, but should serve as a good introduction to the literature in which additional pertinent references may be found. Caution must be observed in relating theoretical band structures to measurements since some of the experiments were done on multiple spin-density-wave crystals, while the theoretical studies have been done mostly on an assumed paramagnetic structure. Nevertheless, it becomes clear below that a reasonable correlation exists between experiment and theory in its present form.

The remainder of this paper is organized as follows. The method of calculation is presented and the band structure is given in Sec. II. The Fermi surface is presented and interpreted in terms of various experiments in Sec. III. Compton profiles and x-ray form factors obtained from the band structure are compared with experiment in Sec. IV, and the optical conductivity is discussed in Sec. V. Section VI contains concluding remarks.

II. BAND STRUCTURE

The technique of calculation used here is reviewed in Ref. 23, and is the same used in recent work on transition metals.[24-26] The Gaussian-orbital basis consisted of 13 s-type, 10 p-type, 5 d-type, and 1 f-type orbitals. The s, p, and d orbital exponents were obtained from the atomic wave functions of Wachters,[49] and the f exponent was assigned the value 0.9 $(\text{a.u.})^{-2}$. The lattice constant was taken to be 5.4456 a.u.

The initial charge density was a superposition of neutral-atom charge densities generated from Wachters's wave functions[49] with a configuration $3d^5 4s$. Two different sets of calculations were made: One employed the Kohn-Sham-Gaspar (KSG) exchange potential[50]; the other used an exchange correlation potential given by von Barth and Hedin (VBH).[51] The iterative cycle was repeated until the change in the leading Fourier coefficients of potential was less than 10^{-4} rydberg, a total of 24 iterations in this case. During these cycles the charge density was obtained from a 140-point sampling in the irreducible wedge of the body-centered-cubic Brillouin zone, which is $\frac{1}{48}$ the volume of the first BZ. The final band structure was generated at 506 points in the wedge. This permitted accurate evaluation of the density of states with the linear-analytic-tetrahedron method.[17]

The band structures which resulted from these calculations are quite similar. The main effect of the use of the VBH exchange correlation is to shift the entire band structure almost rigidly to lower energies by about 0.15 Ry in comparison with those obtained from the KSG potential. Secondarily, there is an overall compression of the band structure by about 8 mRy.

The calculated (KSG) band structure is shown in Fig. 1(a) along symmetry directions; representative energy differences are listed in Table I in comparison with earlier calculations. Fig. 1(a) resembels several of the earlier results for paramagnetic chromium,[6-12] except that levels near the Fermi energy at N appear to be very sensitive to the form of potential as well as the exchange approximation. The calculations which can be most closely compared to this work are shown in Table I.[6-8,10,11] In Ref. 7 Asano and Yamashita applied the Green's-function method to the para- and antiferromagnetic phases of chromium. Their self-consistent calculation included an $X\alpha$ exchange potential with $\alpha = 1$ and an additional correlation correction. A recent band-structure calculation for a commensurate antiferromagnetic phase has been reported by Skriver[52] who employed the same VBH exchange correlation potential used in this work. In Ref. 6 Gupta and Sinha reported an augmented-plane-wave (APW) band structure obtained with an $X\alpha$ exchange with $\alpha = 1$. They did not iterate their potential to self-consistency, and, unless they made an inspired choice for their potential, comparison with the present results is not expected to

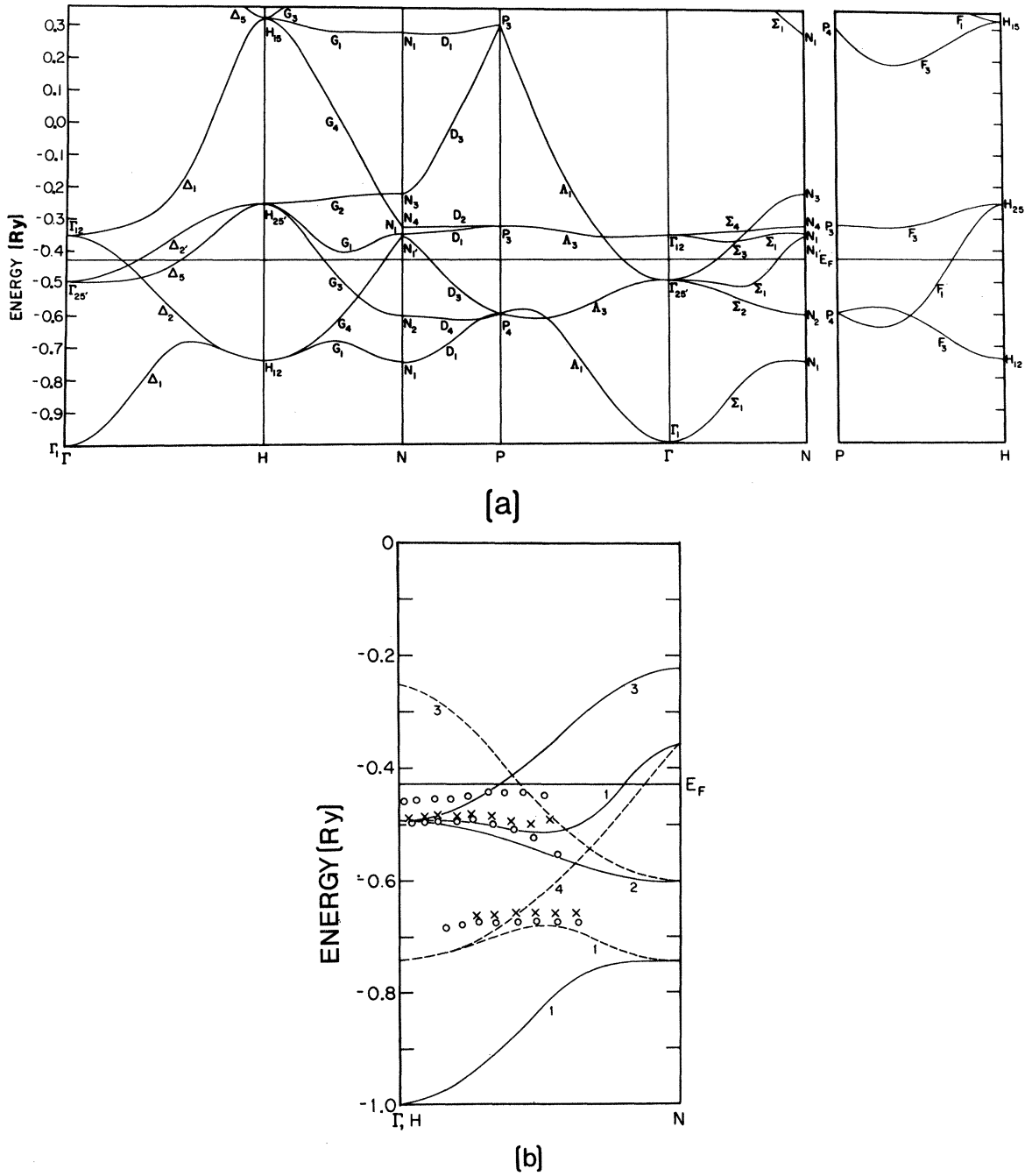

FIG. 1. (a) Energy bands in chromium (KSG potential) along lines of high symmetry. (b) Comparison of the KSG energy bands with angle-resolved photoemission data. The bands from N to H have been folded back over those from Γ to N as an approximation to the antiferromagnetic bands. The solid curves are states of Σ symmetry and the dashed curves are states of G symmetry. Reference 53 is represented by × (75° angle) and ○ (15° angle).

be quantitative. Yasui *et al.*[8] employed a combination of tight-binding and orthogonalized-plane-wave (OPW) methods in self-consistent calculations for two different $X\alpha$ exchange parameters, $\alpha = 1.0$ and $\alpha = 0.725$. They found $\alpha = 0.725$ gave the best Fermi-surface and spin-density wave parameters.

The importance of improvements made in the LCGO method since the earlier calculation of Rath and Callaway[10] can be seen by comparing their results directly in the table. It is thought that the additional variational freedom in this study accounts for most of the differences. The s and p

TABLE I. Selected energy differences (in Ry) for paramagnetic chromium.

	Present (VBH)	Present (KSG)	Ref. 11	Ref. 10	Ref. 7	Ref. 6	Ref. 8
$E_F-\Gamma_1$	0.5599	0.5678	0.7143	0.536	0.5175	0.624	0.500
$\Gamma_{12}-\Gamma_1$	0.6364	0.6454	0.8210	0.6102	0.5785	0.709	0.569
$\Gamma_{12}-\Gamma_{25'}$	0.1440	0.1431	0.1715	0.1590	0.1332	0.136	0.145
$\Gamma_{25'}-\Gamma_1$	0.4924	0.5022	0.6495	0.4513	0.4453	0.573	0.424
$H_{25'}-H_{12}$	0.4801	0.4877	0.6620	0.4812	0.4848	0.523	0.467
$H_{15}-\Gamma_1$	1.3201	1.3201	1.3723	1.2644		1.330	1.097
$H_{25'}-\Gamma_{25'}$	0.2387	0.2411	0.3166	0.2670	0.2341	0.238	0.298
$\Gamma_{12}-H_{12}$	0.3854	0.3897	0.5168	0.3730	0.3840	0.421	0.314
P_3-P_4	0.2719	0.2748	0.3813	0.2670	0.2505	0.300	0.227
N_2-N_1	0.1407	0.1444	0.2089	0.1234	0.1327	0.170	0.109
N_3-N_1	0.5156	0.5235	0.7132	0.5302	0.5025	0.558	0.498
$N_4-N_1(2)$	0.0228	0.0226	0.0343	0.0211	0.0201	0.024	−0.011
$N_{1'}-N_4$	−0.0224	−0.0314	−0.1876	0.0115	0.0531	−0.109	0.074
$N_3-N_{1'}$	0.1219	0.1340	0.3303	0.1087	0.0498	0.215	0.069

basis was expanded and f orbitals were added. The position of the p-type state, N_1', was influenced the most. Note, however, that this position is highly dependent upon the exchange potential chosen (see Table I), leading to more disagreement concerning the relative positions of the states N_1, N_1', and N_4.

The width of the occupied portion of the d bands, measured by E_F-H_{12}, is 4.25 eV for the KSG bands and 4.20 eV for the VBH bands. The corresponding total occupied bandwidths ($E_F-\Gamma_1$), 7.72 eV and 7.62 eV, are slightly larger than the width of about 7 eV found by Johansson *et al.*[53] using angle-resolved photoemission. The total bandwidth including unoccupied states as determined from the $H_{25'}-H_{12}$ difference is 6.63 eV (KSG potential) and 6.53 eV (VBH). McAllister *et al.*[54] estimated the total d-band width to be 6.2 eV on the basis of x-ray emission and appearance potential measurements.

A recent calculation of the band structure of chromium using a Hartree approximation yielded much wider bands than those presented here.[11] In particular the d-band width and total occupied bandwidth from that calculation are 9.0 eV and 9.7 eV, respectively, both unreasonably large values.

Angle-resolved photoemission results recently became available for chormium[53] and agreed reasonably well with the antiferromagnetic bands of Asano and Yamashita. However, the final-state energies used to interpret the electron-energy-distribution curves were obtained from the same Hartree calculation which produced the unreasonable results mentioned earlier. Therefore, we reinterpreted the curves using the usual procedure of fitting a free-electron-like curve to the (KSG) Σ_1 band which lies in the correct range of photon energies. The results, shown in Fig. 1(b), are in reasonable agreement with our bands and, interestingly enough, are not very different from the results using the Hartree bands. The bands along the G axis ($\bar{N}\bar{H}$) were folded back over those along the Σ axis ($\bar{\Gamma}\bar{N}$) as an approximation to the (commensurate) antiferromagnetic bands since the pertinent photoemission data were obtained for the antiferromagnetic state.

The density of states shown in Fig. 2 is very similar to that obtained in Refs. 8 and 11 and virtually identical to that of Rath and Callaway.[10] A quantity directly related to the density of states at the Fermi energy, $N(E_F)$, is the electronic specific heat. $N(E_F)=9.14$ states/rydberg atom, (9.41 for the VBH potential) which yields a theoretical value for the temperature coefficient of specific heat for electrons of $\gamma=1.58$ (1.62) mJ/mole K^2. Since measurement of this contribution to the specific heat must be performed at low temperature where pure chromium is antiferromagnetic, the experimental value[55] 1.5 mJ/mole K^2, should not be compared directly with this result. In antiferromagnetic chromium the gap induced in the paramagnetic band structure may substantially reduce $N(E_F)$ since large portions of the Fermi surface may disappear. Asano and Yamashita esti-

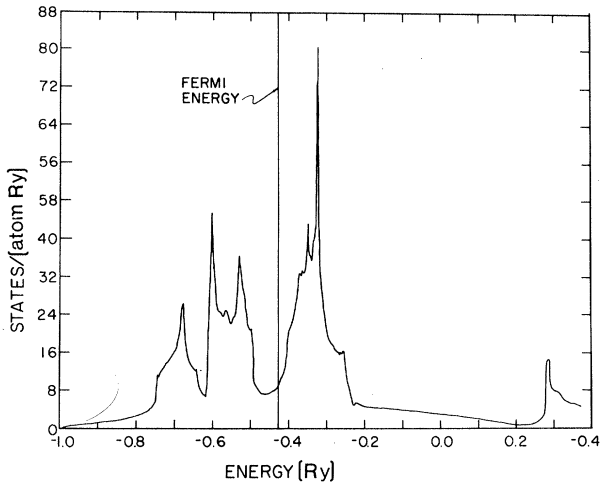

FIG. 2. Density of states of chromium.

mate a 29% reduction of $N(E_F)$, so assuming the same reduction here, a γ value of 1.06 in J/mole K^2 is obtained. Comparison with the experimental value of 1.5 mJ/mole K^2 yields a phonon enhancement factor of $(1+\lambda)=1.50$. Alternatively, one may compare with the paramagnetic specific heat deduced by extrapolating data on paramagnetic alloys of chromium[55]: 2.9 mJ/mole K. From this number one gets $(1+\lambda)=1.83$, which is larger than the previous estimate. A previous calculation[24] for V gave $1+\lambda=2.3$.

III. FERMI SURFACE

The Fermi energy for the self-consistent energy bands is $E_F=0.428$ Ry, shown as a solid line in Fig. 1(a). This energy falls just above the band intersections along the Δ axis and below the N_1' level. The Fermi-surface shapes are shown in Fig. 3. Numbering bands starting with the 4s Γ_1 level as band one, the first two bands are completely filled, band three has hole surfaces at H and N [Fig. 3(b)], band four is the electron "jack" [Fig. 3(a)], and band five is a set of very small electron "lenses" or "hats" (not shown). Cross sections of all three portions of the Fermi surface are shown in Figs. 4 and 5 which are (001) and (011) cross sections passing through Γ. This Fermi surface is similar to that of Ref. 11, except for appearance of holes at N which are a consequence of the exchange potential employed here. There is a remarkable resemblance to the model proposed by Lomer[1] and sketched by Mattheis.[56]

A comparison with various experimental data is summarized in Table II. There is rather good correspondence between the phonon anomalies seen by Muhlstein[36-38] and the Fermi-surface nestings and extremal dimensions.[57] However, the transverse anomaly along the [001] direction seems to fit the extremum dimension of the electron jack along the Δ axis better than the nesting along $\bar{\Gamma}\bar{N}$ as Muhlstein proposed.

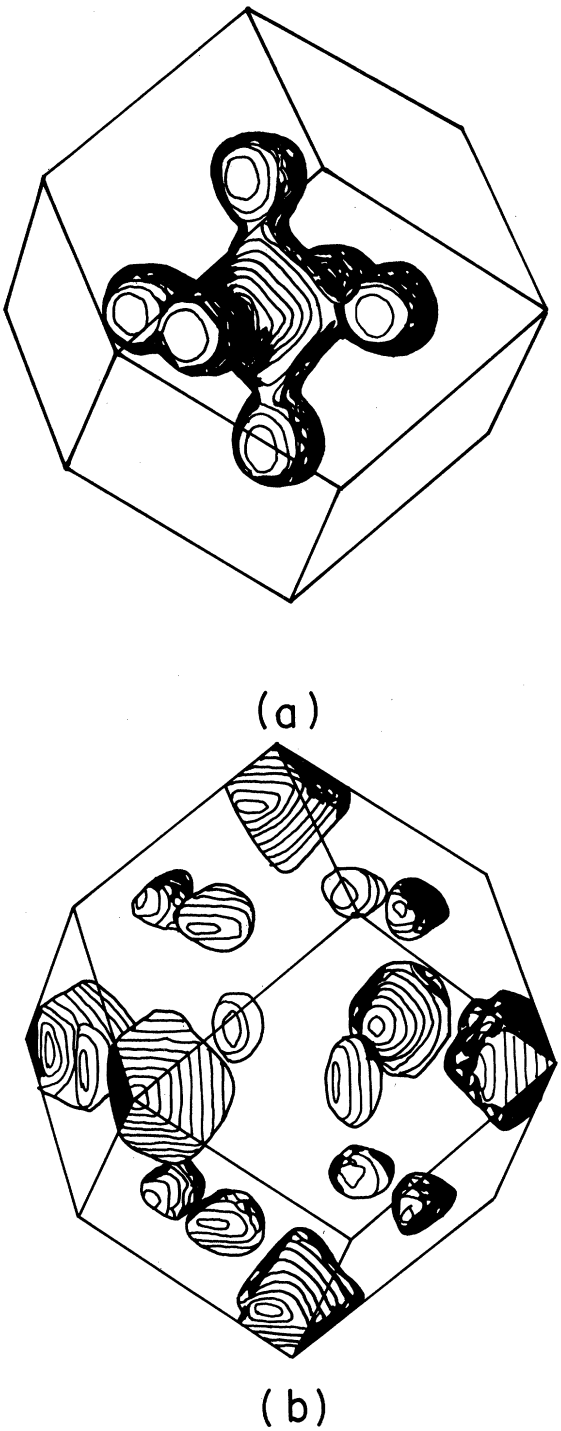

FIG. 3. Fermi surface of chromium. (a) Electron "jack"; (b) hole surfaces near H and N.

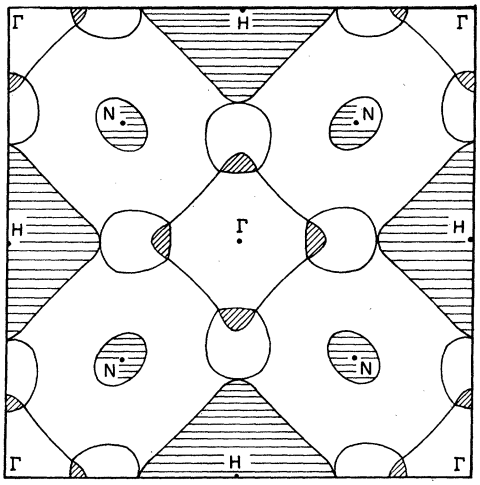

FIG. 4. Fermi-surface cross section: (001) plane.

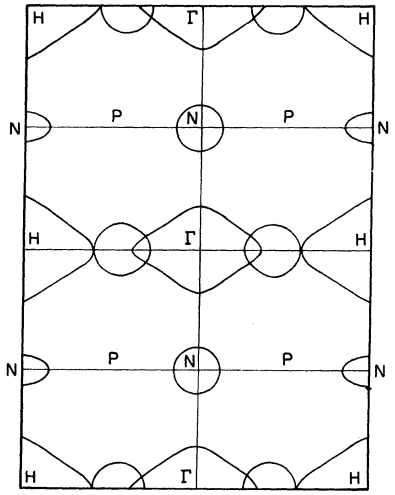

FIG. 5. Fermi-surface cross section: (011) plane.

A. Spin-density wave vector

The spin-density wave is assumed to come from nesting of the body of the electron jack with the hole surface at H (see Table II). The phonon data are not accurate enough or have enough resolution to pick out a Kohn anomaly in the $\bar{\Gamma}\bar{N}$ direction. Possibly the magnon-phonon interaction is involved in this direction to obscure this region. However, it is certain that a spin-density wave does exist[28-29] with a wave vector corresponding to the $\bar{\Gamma}\bar{H}$ nesting. While comparison in Table II is good, a theoretical prediction based upon a full calculation of the magnetic susceptibility $\chi(q)$, preferably followed by a self-consistent band calculation including the spin ordering to see if, indeed, the spin-

TABLE II. Fermi-surface dimensions compared with experimentally deduced values. The phonon data were taken from Refs. 36–38. The spin-density wave vector is found in Refs. 28 and 29. The de Haas-van Alphen data are from Ref. 47.

Fermi-surface feature	Experiment	Expt. Value	Theoretical value KSG	VBH
$\bar{\Gamma}\bar{P}$ extremum of electron jack	Phonon anomaly along $\bar{\Gamma}\bar{P}$	0.25(111)	0.27(111)	0.26(111)
$\bar{\Gamma}\bar{H}$ extremum of electron jack	Phonon anomaly along $\bar{\Gamma}\bar{H}$ near H	0.85(001)	0.82(001)	0.83(001)
Nesting of jack body and hole at N	Phonon anomaly along $\bar{\Gamma}\bar{N}$	0.45(011)	0.42(011)	0.42(011)
Nesting of jack balls and holes at N ($\bar{\Gamma}\bar{P}\bar{H}$ translation)	Phonon anomaly near P	0.54(111)	0.54(111)	0.54(111)
Nesting of jack body and hole at H ($\bar{\Gamma}\bar{P}\bar{H}$ translation)	Phonon anomaly along $\bar{P}\bar{H}$ near H	0.94(111)	0.98(111)	0.99(111)
Nesting of jack body and holes at H ($\bar{\Gamma}\bar{H}$ translation)	Spin-density wave	0.96(001)	0.95(001)	0.96(001)
Dimensions of hole at N	dHvA			
NH		0.173 Å^{-1}	0.186 Å^{-1}	0.185 Å^{-1}
$N\Gamma$		0.234	0.304	0.310
NP		0.268	0.316	0.324
Dimensions of ball at X	dHvA			
ΓH		0.26 Å^{-1}	0.30 Å^{-1}	0.30 Å^{-1}
$\perp\Gamma H$		0.25	0.30	0.30

density wave is the ground-state configuration. From Refs. 6 and 7 it is expected that such studies would not alter the estimated values greatly.

B. de Hass-van Alphen data

The Fermi-surface cross-section areas quoted in Table II were obtained from the de Haas–van Alphen measurements of Graebner and Marcus.[47] In that work, the dimensions of ellipsoids at X (electron balls) and at N (hole surfaces) were chosen to provide the best fit to observed dHvA frequencies. The quoted dimensions reproduced the dHvA frequencies to within 10% for the balls at X and 20% for the holes at N. Dimensions given in Table II for the hole surfaces were deduced from the figures in Ref. 47 since they were not quoted there. A direct comparison of the areas calculated from the theoretical band structure with the dHvA data might remove some of the differences shown in Table II. One could also attribute these differences to changes which occur in the Fermi surface in the presence of the spin-density wave, but then another argument would be needed to explain the apparent good agreement with the other data. One should also consider to what extent a local exchange approximation can be expected to produce Fermi surfaces in agreement with experimental values.[58]

IV. X-RAY FORM FACTORS AND COMPTON PROFILE

Table III contains the x-ray form factors from the self-consistent paramagnetic band structure of chromium (KSG potential). Also included are the values of Rath and Callaway[10] and Wakoh and Yamashita,[12] along with various experimental results. The experimental and theoretical values are in reasonable agreement, in view of the large differences between the results of different experimental groups (compare Refs. 41 and 42 with 43).

The LCGO wave functions have also been employed to compute the Compton profile, $J_{\hat{k}}(q)$, for paramagnetic chromium. Procedures discussed by Rath *et al.*[59] were used to determine the part of $J_{\hat{k}}(q)$ contributed by the band electrons ($3d$ and $4s$) for three symmetry directions. These are given in Table IV along with the directional average for a range of q values. The spherically averaged profile is compared with the experimental results of Paakkari, Manninen, and Berggren[39] in Fig. 6. The contribution from the core electrons was calculated by Weiss *et al.*[60] in the Hartree-Fock approximation. This has been subtracted from the experimental data before plotting. Figure 7 displays the calculated anisotropy of the profile. The experimental results are obtained from Weiss.[40] The experimental anisotropy is rather small, both theoretical and experimental estimates may not be too reliable.

TABLE III. X-ray form factors for paramagnetic chromium.

Wave vector $aK/2\pi$	Present	Ref. 10	Ref. 12	Ref. 41	Ref. 42	Ref. 43
(1,1,0)	16.29	16.27	16.32	15.88	15.78 ± 0.20	16.30 ± 0.12
(2,0,0)	13.39	13.31	13.46	13.14 ± 0.34	13.13 ± 0.17	
(2,1,1)	11.66	11.60	11.56	11.23 ± 0.34	11.47 ± 0.15	
(2,2,0)	10.39	10.33	10.27	9.97 ± 0.50	10.20 ± 0.14	
(3,1,0)	9.40		9.36	8.94 ± 0.30		
(2,2,2)	8.82		8.70	8.44 ± 0.16		
(3,2,1)	8.27		8.20	7.75 ± 0.10		
(4,0,0)	7.76		7.81	7.50 ± 0.24		
(3,3,0)	7.54	7.510		7.05 ± 0.09		
(4,1,1)	7.48	7.448				
(4,2,0)	7.23			6.72 ± 0.15		
(3,3,2)	7.06			6.59 ± 0.19		
(4,2,2)	6.84			6.41 ± 0.12		
(4,3,1)	6.66			6.28 ± 0.09		
(5,1,0)	6.59					
(5,2,1)	6.33			5.96 ± 0.11		
(3,3,0)/(4,1,1)	1.008	1.008			1.013 ± 0.007	
(4,4,2)/(6,0,0)	1.014				1.014 ± 0.007	

TABLE IV. Calculated Compton-profile function $J_{\hat{k}}(q)$ for the [1,0,0], [1,1,0], and [1,1,1] directions and the spherical average.

q	J_{100}	J_{110}	J_{111}	J_{av}
0.0	2.103	2.277	2.574	2.304
0.1	2.104	2.268	2.536	2.290
0.2	2.052	2.207	2.360	2.202
0.3	2.003	2.139	2.134	2.099
0.4	1.968	2.033	1.916	1.984
0.5	1.899	1.880	1.755	1.853
0.6	1.799	1.724	1.623	1.720
0.7	1.701	1.591	1.510	1.602
0.8	1.547	1.472	1.427	1.482
0.9	1.417	1.357	1.340	1.370
1.0	1.286	1.232	1.258	1.254
1.2	0.997	0.984	0.904	0.967
1.4	0.745	0.713	0.645	0.705
1.6	0.611	0.555	0.630	0.590
1.8	0.425	0.449	0.482	0.450
2.0	0.359	0.372	0.374	0.369
2.5	0.276	0.263	0.248	0.263
3.0	0.143	0.159	0.188	0.162
3.5	0.111	0.104	0.096	0.104
4.0	0.066	0.068	0.063	0.066
4.5	0.044	0.046	0.044	0.045
5.0	0.031	0.030	0.031	0.030

V. OPTICAL CONDUCTIVITY

The optical conductivity of chromium has been measured by Nestell and Christy[35] and by Ganin *et al.*[33] A comparison between these experimental results and various forms of the optical conductivity computed from this band structure are shown in Fig. 8. Curve A was computed from the KSG bands using the analytic tetrahedron method[16,17] and the full $\vec{k}$ dependence of the matrix elements for interband transitions only. In the computations, contributions from various bands were not separated in order to speed up the calculations and simplify computer codes, so it is not possible to make assignments of peaks to particular transitions with much certainty. However, it is probable that the 1.2-eV peak is a $\Delta_5 \rightarrow \Delta_2'$ transition which has a threshold of 1 eV. A peak has been observed in thermoreflectance measurements near this energy.[34] The peak near 1.9 eV is probably associated with $\Delta_5 \rightarrow \Delta_1$ and $\Sigma_1 \rightarrow \Sigma_4$ transitions. Structure in this range has also been reported in thermoreflectance. The contributions to both the broad main peak and the smaller one near 6.3 eV appear to come from several regions of the Brillouin zone.

The experimental curves, unfortunately, do not reveal much structure. Presumably this is a result of lifetime broadening. In order to compare with experiment, an empirical lifetime broadening of 0.5 eV and the intraband (Drude) contributions were included (curve B).[61] To obtain better agreement, a self-energy correction[62,63] was also included (curve C), with the parameter λ chosen so that the 6.3-eV theoretical peak coincided with the 5.9-eV peak in the experimental data. This

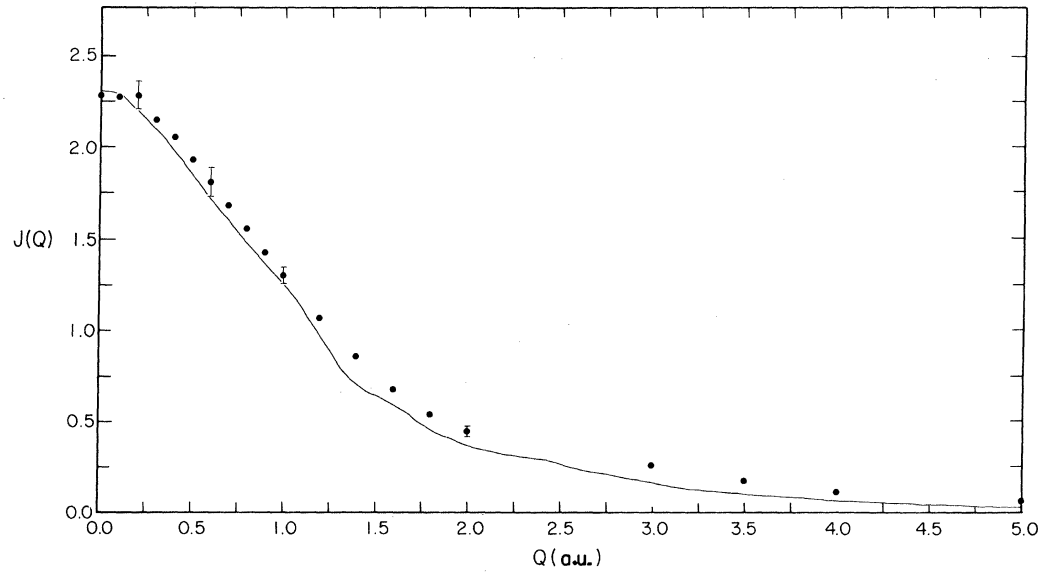

FIG. 6. Spherically averaged Compton profile. The experimental points are from Ref. 39.

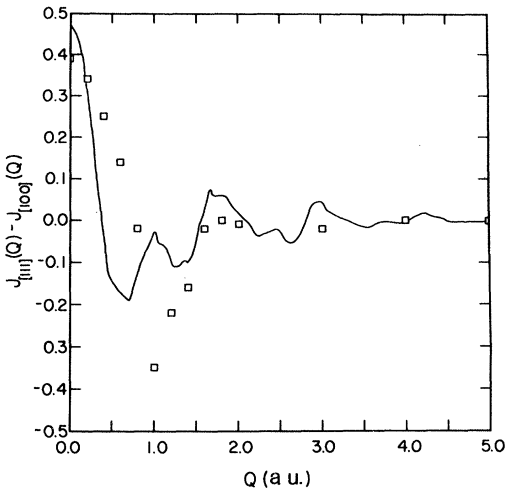

FIG. 7. Anisotropy of the Compton profile. The experimental points are from Ref. 40.

required $\lambda = 0.1$ the same as that found[63] in the case of iron ($\lambda = -0.1$) and close to the value for nickel ($\lambda = -0.12$). However, the calculated position of the main peak remains somewhat too high even with this adjustment. There also remain some differences in the magnitudes of the peaks. Resolution of these differences may require more sophisticated self-energy corrections or the adoption of a nonlocal exchange potential.

VI. CONCLUSIONS

The LCGO method has been used to perform a self-consistent calculation of the energy bands in paramagnetic chromium using both the Kohn-Sham-Gaspar and the von Barth–Hedin exchange potentials. The Fermi-surface and x-ray form factors were the same to within 2% and hence the Compton profiles and optical conductivity were obtained for the Kohn-Sham potential alone. Comparisons have been made with experimental data. In general, the agreement between theory and experiment is fairly good in regard to Fermi-surface properties (which are, however, not particularly sensitive to details of the potential). There are still difficulties in regard to x-ray form factors, which are probably experimental. The Compton profile is quite satisfactory. The comparison of theoretical and experimental optical conductivities shows features common to other transition metals, in particular large lifetime broadening at high energies and an apparent compression (about 10%) of the d-band states.

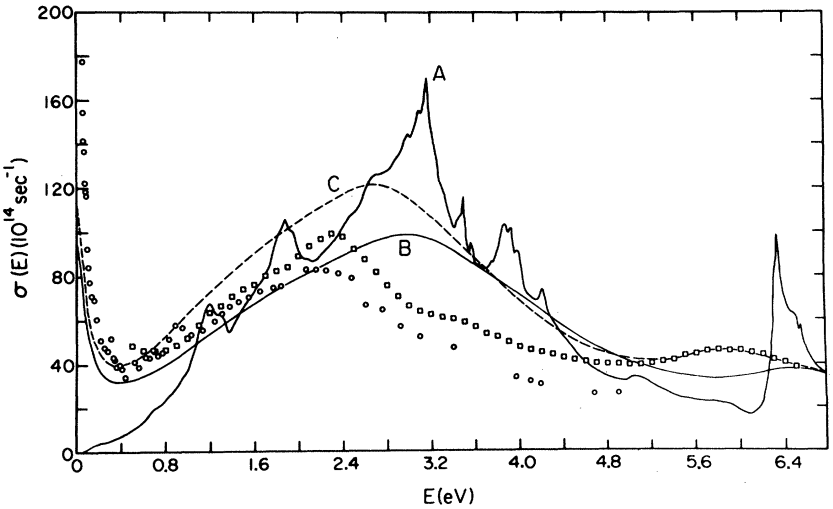

FIG. 8. Optical conductivity of chromium. Curves: A, interband conductivity assuming sharp band states; B, including a relaxation time $\hbar/\tau = 0.5$ eV and a free-electron (Drude) contribution; C, including a "self-energy" correction. Reference 33 is represented by ○, Ref. 35 by □.

ACKNOWLEDGMENTS

The portion of this work done at Louisiana State University was supported by the National Science Foundation. Work done at UTA University of Texas at Arlington was supported by the Robert A. Welch Foundation and by the Air Force Office of Scientific Research.

[1]A. W. Overhauser, Phys. Rev. Lett. 4, 462 (1960); Phys. Rev. 128, 1437 (1962).
[2]W. M. Lomer, Proc. Phys. Soc. London 80, 489 (1962); 84, 327 (1964).
[3]C. Herring, in *Magnetism*, edited by G. Rado and H. Suhl (Academic, New York, 1966), Vol. 4.
[4]J. Callaway, *Quantum Theory of the Solid State* (Academic, New York, 1974).
[5]L. M. Roth, H. J. Zeiger, and T. A. Kaplan, Phys. Rev. 149, 519 (1966).
[6]R. P. Gupta and S. K. Sinha, Phys. Rev. B 3, 2401 (1971); see also K. H. Oh, B. N. Harmon, S. H. Liu, and S. K. Sinha, Phys. Rev. 14, 1283 (1976).
[7]A. Asano and J. Yamashita, J. Phys. Soc. Jpn. 23, 714 (1967).
[8]M. Yasui, E. Hayashi, and M. Shimizu, J. Phys. Soc. Jpn. 29, 1446 (1970).
[9]J. D. Connolly, Intern. J. Quantum Chem. 25, 257 (1968).
[10]J. Rath and J. Callaway, Phys. Rev. B 8, 5398 (1973).
[11]J. L. Fry, N. E. Brener, J. L. Thompson, and P. H. Dickinson, Phys. Rev. B 21, 384 (1980).
[12]S. Wakoh and J. Yamashita, J. Phys. Soc. Jpn. 35, 1394 (1973).
[13]L. L. Boyer, D. A. Papaconstantopoulos, and B. M. Klein, Phys. Rev. B 15, 3685 (1977).
[14]J. Callaway and C. S. Wang, Phys. Rev. B 7, 1096 (1973).
[15]E. C. Snow, Phys. Rev. 171, 785 (1968).
[16]S. P. Singhal, Phys. Rev. B 12, 564 (1975).
[17]J. Rath and A. J. Freeman, Phys. Rev. B 11, 2109 (1975).
[18]N. E. Brener and J. L. Fry, Phys. Rev. B 19, 1720 (1979).
[19]N. E. Brener and J. L. Fry, Intern. J. Quantum Chem. 14S, 455 (1980).
[20]J. Callaway and A. K. Chatterjee, J. Phys. F 8, 2569 (1978).
[21]J. T. Devreese, F. Brosens, and L. F. Lemmens, Phys. Rev. B 21, 1349 (1980); 21, 1363 (1980).
[22]J. Callaway and J. L. Fry, in *Computational Methods in Band Theory*, edited by P. M. Marcus, J. F. Janak, and A. R. Williams (Plenum, New York, 1971), p. 571.
[23]C. S. Wang and J. Callaway, Comput. Phys. Commun. 14, 327 (1978).
[24]D. G. Laurent, C. S. Wang, and J. Callaway, Phys. Rev. B 17, 455 (1978).
[25]C. S. Wang and J. Callaway, Phys. Rev. B 15, 298 (1977).
[26]J. Callaway and C. S. Wang, Phys. Rev. B 16, 2095 (1977).
[27]Yu. N. Smirnov and V. A. Finkel, Zh. Eksp. Teor. Fiz. 47, 476 (1964) [Sov. Phys.–JETP 20, 315 (1965)].
[28]R. M. Moon, W. I. Koehler, and A. L. Trego, J. Appl. Phys. 37, 1036 (1966).
[29]W. Koehler, R. M. Moon, A. L. Trego, and A. R. Mackintosh, Phys. Rev. 151, 405 (1966).
[30]C. Stassis, G. R. Kline, and S. R. Sinha, Phys. Rev. Lett. 31, 1498 (1973); Phys. Rev. B 11, 2171 (1975).
[31]S. K. Sinha, G. R. Kline, C. Stassis, and N. Chesser, Phys. Rev. B 15, 1415 (1977).
[32]A. S. Barker, Jr. and J. A. Ditzenberger, Phys. Rev. B 1, 4378 (1970).
[33]G. V. Ganin, M. M. Kirillova, L. V. Nomerovannaya, and V. P. Shirokovskiy, Fiz. Met. Metalloved. 43, 907 (1977) [Phys. Met. Metallogr. (USSR) 43, 4 (1977)].
[34]J. H. Weaver, D. W. Lynch, C. H. Culp, and R. Rosei, Phys. Rev. B 14, 459 (1976).
[35]J. E. Nestell, Jr. and R. W. Christy, Phys. Rev. B 21, 3173 (1980).
[36]W. M. Shaw and L. D. Muhlestein, Phys. Rev. B 4, 969 (1971).
[37]L. D. Muhlestein, E. Gürmen, and R. M. Cunningham, in *Inelastic Scattering of Neutrons* (IAEA, Grenoble, 1972), p. 53.
[38]L. D. Muhlestein, E. Gurmen, and R. M. Cunningham, in *Proceedings of 18th Annual Conference on Magnetism and Magnetic Materials*, edited by C. D. Graham and J. J. Rhyne (American Institute of Physics, New York, 1972).
[39]T. Paakkari, S. Manninen, and K. F. Berggren, Phys. Fenn. 10, 207 (1975).
[40]R. J. Weiss, Philos. Mag. 27, 1461 (1973).
[41]M. J. Cooper, Philos. Mag. 7, 2059 (1962); 10, 177 (1964).
[42]M. Diana and G. Mazzone, Phys. Rev. B 5, 3832 (1972).
[43]M. Fujimoto, O. Terasaki, and D. Watanabe, Phys. Lett. 41A, 159 (1972).
[44]M. O. Steinitz, E. Fawcett, C. E. Burleson, J. A. Schaefer, L. O. Frishman, and J. A. Marcus, Phys. Rev. B 5, 3675 (1972).
[45]R. Griessen and E. Fawcett, J. Phys. F 7, 2141 (1977).
[46]A. J. Arko, J. A. Marcus, and W. A. Reed, Phys. Rev. 176, 671 (1968).
[47]J. E. Graebner and J. A. Marcus, Phys. Rev. 175, 659 (1968).
[48]S. Kotani and N. Mori, Solid State Commun. 27, 1013 (1978).
[49]A. J. H. Wachters, J. Chem. Phys. 52, 1033 (1970).
[50]W. Kohn and L. J. Sham, Phys. Rev. 140, A1133 (1965); R. Gaspar, Acta Phys. Hungary 3, 263 (1954).
[51]U. von Barth and L. Hedin, J. Phys. C 5, 1629 (1972).
[52]H. L. Skriver, J. Phys. F 11, 97 (1980).
[53]L. I. Johansson, L. G. Peterson, K.-F. Berggren, and J. W. Allen, Phys. Rev. B 22, 3294 (1980).
[54]A. J. McAllister, J. P. Cuthill, R. C. Dobbyn, M. L. Williams, and R. E. Watson, Phys. Rev. B 12, 2973 (1975).

[55]P. Heiniger, E. Bucher, and J. Mueller, Phys. Kondens. Mater. 5, 243 (1966).
[56]L. F. Mattheis, Phys. Rev. 139, A1893 (1965).
[57]This analysis is based upon the considerations of Ref. 5. A more accurate prediction requires calculation of $\chi(q)$, and matrix-element or volume effects may be important. A good discussion is given by Michele Gupta and A. J. Freeman, Phys. Rev. B 14, 5205 (1976).
[58]S. B. Nickerson and S. H. Vosko, Phys. Rev. B 14, 4399 (1976).
[59]J. Rath, C. S. Wang, R. A. Tawil, and J. Callaway, Phys. Rev. B 8, 5139 (1973).
[60]R. J. Weiss, A. Harvey, and W. C. Phillips, Philos. Mag. 17, 241 (1968).
[61]A. P. Lenham and D. M. Treherne, in *Optical Properties and Electronic Structure of Metals and Alloys,* edited by F. Abeles (North-Holland, Amsterdam, 1966), p. 196.
[62]J. F. Janak, A. R. Williams, and V. L. Moruzzi, Phys. Rev. B 11, 1522 (1975).
[63]D. G. Laurent, J. Callaway, and C. S. Wang, Phys. Rev. B 20, 1134 (1979).